

# Time-Interleaving Enabled Co-propagation of QKD with a 10-dBm 100-Gb/s QPSK Channel over 100-km Fiber

Jing Wang<sup>(1)\*</sup>, Brian J. Rollick<sup>(1)\*</sup>, Zhensheng Jia<sup>(1)</sup>, Haipeng Zhang<sup>(1)</sup>, Bernardo A. Huberman<sup>(1)</sup>

<sup>(1)</sup> CableLabs, 858 Coal Creek Circle, Louisville, CO, 80027.

\* These authors contributed equally. [j.wang@cablelabs.com](mailto:j.wang@cablelabs.com), [b.rollick@cablelabs.com](mailto:b.rollick@cablelabs.com)

**Abstract** By time-interleaving QKD pulses into gaps between classical data frames, we experimentally demonstrate the C-band co-propagation of a polarization-encoding decoy-state BB84 QKD channel and a 10-dBm 100 Gb/s QPSK channel over 100-km fiber with minimum Raman noise interference.

## Introduction

Quantum key distribution (QKD) provides information-theoretic security<sup>[1],[2]</sup> and is a solution to the cybersecurity threats of quantum computing<sup>[3],[4]</sup>. So far, most QKD systems use dedicated/dark fibers due to the spontaneous Raman scattering (SpRS) noise from classical data channels. But it is cost-prohibitive to add new fibers or reserve dedicated fibers for quantum communications. The only chance for the commercial success of QKD technologies is integration into existing fiber networks and sharing fibers with classical data traffic.

There have been several QKD/classical coexistence solutions developed. One method is to move the QKD channel to the O-band<sup>[5]</sup>. Thanks to the large wavelength separation, this method significantly reduces the SpRS noise<sup>[6]</sup> and enables coexistence with Tb/s classical data traffic with launch power of more than 20 dBm<sup>[7]–[10]</sup>. But the high fiber loss in the O-band limits the fiber distance to less than 80 km<sup>[6]</sup>, even using G.654 ultra-low loss fibers<sup>[7],[9]</sup>. Network compatibility is another issue since most deployed optical routers only support C-band operations. Another method is the C-band coexistence with attenuated classical channels<sup>[11]</sup>. This method only works for low data rate communications<sup>[12]–[18]</sup>, where there is plenty of power margin so classical channels can be attenuated to matching receiver sensitivities. For 100 Gb/s and beyond, normal QKD operation is impossible unless the classical channel is attenuated below receiver sensitivities<sup>[19]</sup>. This method trades the performance of classical channels for lower SpRS noise and will not work in real deployments since attenuated classical channels will not meet the distances or BER requirements.

In this paper, we use time-interleaving techniques to embed QKD pulses into the gaps between classical data frames and experimentally

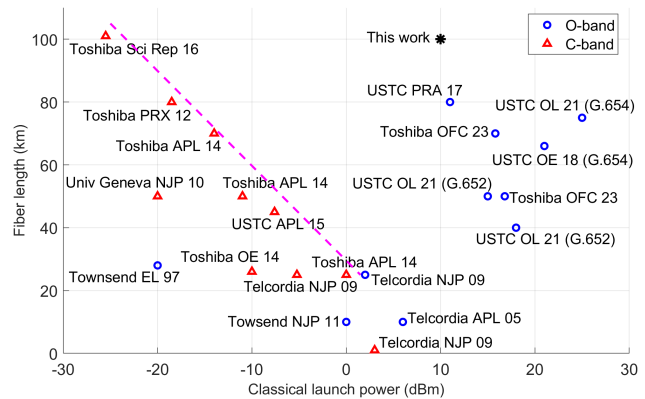
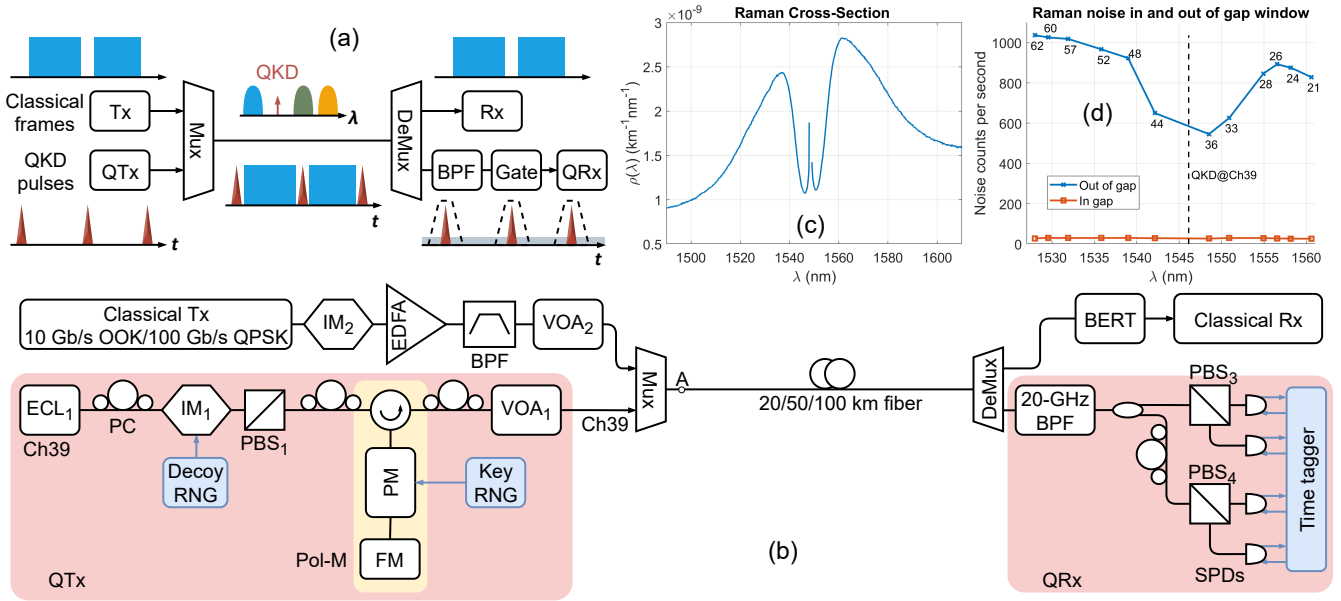


Fig. 1: State-of-the-art of QKD/classical coexistence.

demonstrate the co-propagation of a polarization-encoding decoy-state BB84 QKD channel with a 10-dBm 100-Gb/s QPSK channel over 100 km of fiber. Our method leverages the low fiber loss of the C-band while removing the power limit of classical channels, enabling co-propagation without sacrificing the performance of either QKD or classical channels. Fig. 1 shows the state-of-the-art coexistence works in terms of the maximum fiber distance of QKD channels and the maximum power allowed for classical channels. O-band results are labeled by blue circles, which allow Tb/s and high-power classical communications but are bounded to 80 km. The C-band results are labeled by red triangles, which are all below a dashed line, showing a trade-off between QKD distances and classical channel power. Our result, labeled by a star, is the only outlier above the trade-off limit.

## Operation Principles

The operation principles of the time-interleaving technique are shown in Fig. 2(a). The QKD and classical channels use two different wavelengths in the C-band. QKD pulses are embedded into the gaps between classical data frames. After fiber propagation, QKD and classical channels can be separated in both wavelength and time



**Fig. 2:** (a) Operation principles. (b) Experimental setup. (c) Raman cross-section. (d) Noise counts in and out of gap windows.

domains using spectral filtering and temporal gating, respectively. A narrow bandpass filter (BPF) blocks the out-of-band SpRS noise and gated SPDs eliminate the out-of-window noise.

### Experimental Setup

Fig. 2(b) shows the experimental setup. We build a polarization-encoding decoy-state BB84 QKD system with a center wavelength of 1546.12 nm (ITU-T Ch39, 193.9 THz). The intensity modulator ( $IM_1$ ) generates pulses and prepares decoy states. The pulse width is 200 ps with a 25 MHz repetition rate. The polarization modulator (Pol-M) consists of a circulator, a phase modulator (PM), and a Faraday mirror (FM)<sup>[20]–[22]</sup>. A variable optical attenuator ( $VOA_1$ ) controls the pulse intensity at point A at single-photon levels. An optical switch selects one out of the two classical channels, 10 Gb/s OOK or 100 Gb/s QPSK, to be interleaved with the QKD channel. The classical channel wavelength is tunable across the C-band. To emulate gaps between classical data frames,  $IM_2$  carves 15-ns gaps on continuous data traffic. An EDFA and  $VOA_2$  control the classical channel power. The classical launch power at point A is 10 dBm, which is at least one order of magnitude higher than other C-band works<sup>[15]–[19]</sup>. Three fiber lengths, 20, 50, and 100 km, are tested, with 10 Gb/s OOK for 20 and 50 km fibers, and 100 Gb/s QPSK for 100 km fiber. The QKD synchronization channel is omitted since a 25 MHz optical clock signal has too low power to impact the QKD performance. The classical and quantum channels are mux/demux by 100-GHz DWDMs. A 20-GHz narrowband filter is used to block the out-

of-band noise. Single-photon detectors (SPDs) work in gated mode with a 4-ns gate width to eliminate out-of-window noise. The SPDs have 20% detection efficiency, 10  $\mu$ s dead time, and a dark count rate of 6e-6 per gate. The optical misalignment is 0.5-1%. We use a three-intensity decoy-state protocol with mean photon numbers per pulse of 0.85, 0.04, and 1e-3 for signal, decoy, and vacuum states, and emission probabilities of 0.9, 0.05, and 0.05, respectively.

### Results

Fig. 2(c) shows the measured Raman cross-section of a classical channel at 1548.52 nm (Ch36, 193.6 THz). To reveal the fine spectral structure of SpRS noise, the central peak of the pump wavelength is removed. Two local minima are located 200-300 GHz away from the pump wavelength on both sides. The anti-Stokes noise on the shorter wavelength side is smaller. To validate the effectiveness of SpRS noise suppression in gap windows, noise count rates in and out of the gap window are shown in Fig. 2(d). The noise counts out of the gap window show a similar wavelength dependence as the Raman cross-section; but inside the gap window, noise counts are kept low for all classical wavelengths.

Three co-propagation scenarios are tested in the experiments. QKD with 10 Gb/s OOK over 20 and 50 km fiber, and QKD with 100 Gb/s QPSK over 100 km fiber. Fig. 3 shows quantum bit error rates (QBER) and secure key rates (SKR) as functions of the classical channel launch power. Since our key rates are limited by the slow response and long dead time of low-cost SPDs,

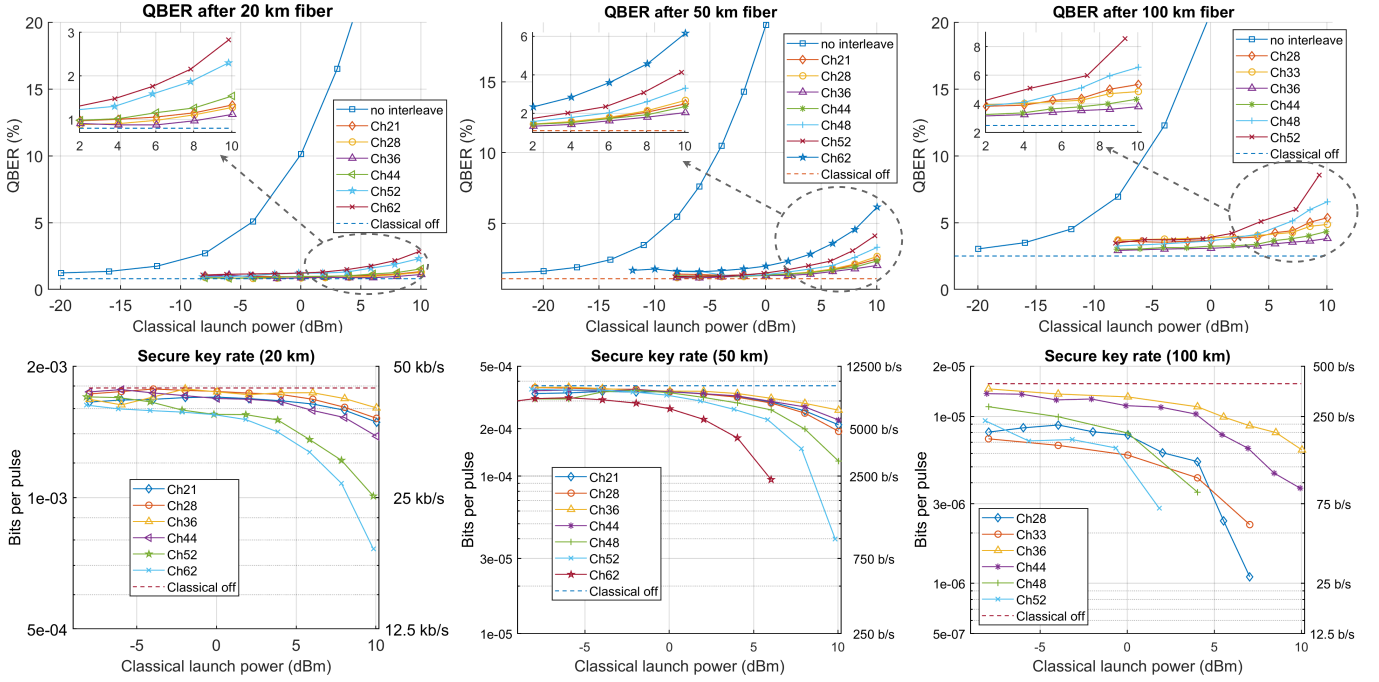


**Fig. 3:** QBER and SKR vs classical launch power. (a, b) 20 km. (c, d) 50 km. (e, f) 100 km.

the key rates are shown in both bits per pulse and bits per second. Since time-interleaving allows continuous QKD operation without interruption, we followed the asymptotic case of infinite decoy states<sup>[23]</sup> for key rate estimation. With the QKD channel fixed at 1546.12 nm (Ch39, 193.9 THz), the classical channel is tuned across the C-band to investigate the wavelength dependence of SpRS noise.

Fig. 3(a, b) show the 20 km case, (c, d) for the 50 km case, and (e, f) for the 100 km case. Without time-interleaving, QBER increases rapidly with classical power. The dashed line shows the QBER with the classical channel turned off. Time-interleaving effectively suppresses the SpRS noise in the gap window, so QBER increases much slower with classical power, as shown in the insets. The QKD performance shows a wavelength selectivity for the classical channel. The best place to put a classical channel is at Ch36 (193,6 THz, 1548.52 nm) so that the QKD channel at Ch39 is within the minimum of SpRS noise. QBER of 1.12%, 2.04%, 3.81% and SKRs of  $1.6 \cdot 10^{-3}$  (40 kb/s),  $2.63 \cdot 10^{-4}$  (6.6 kb/s), and  $6.3 \cdot 10^{-6}$  (157 b/s) are archived for 20, 50, and 100 km fibers. But for wavelengths far away from the quantum channel, QKD performance deteriorates quickly with fiber distance. At 50 km, no secure key is generated if the classical channel is at Ch62. At 100 km, the wavelength range of classical channels that allows QKD operation is from -300 GHz to +500 GHz (Ch36 to Ch44). This

is due to the dispersion walk-off effect. Raman scattering converts the photons from the classical wavelength  $\lambda_C$  to the quantum wavelength  $\lambda_Q$ . A photon travels at the speed of  $\lambda_C$  before the conversion, and at the speed of  $\lambda_Q$  afterward. Due to fiber dispersion,  $\lambda_C$  and  $\lambda_Q$  have different speeds, so noise photons generated at different locations will arrive asynchronously at the fiber end. As the SpRS noise is spread in the time domain, the initial 15-ns gap window shrinks and noise sneaks into the gating window of SPDs. Longer fiber distance and larger wavelength separation between the two interleaved channels lead to more severe walk-off.

## Conclusions

We experimentally demonstrated a time-interleaving technique that enables the C-band co-propagation of QKD with a 10-dBm 100 Gb/s QPSK channel over 100 km of fiber. Our method leverages the low fiber loss in the C-band while removing the power limit of classical channels, enabling co-propagation without sacrificing either performance. Compared with other C-band results, our 10-dBm launch power is at least one order of magnitude higher. Although time-interleaving cannot be used for counter-propagation scenarios, it is still useful since most deployed fiber networks use one fiber in each direction. While we only demonstrated one classical channel in this work, time-interleaving can also be applied to multiple classical channels with appropriate wavelength planning.

## References

- [1] N. Gisin, G. Ribordy, W. Tittel, and H. Zbinden, "Quantum cryptography", *Rev. Mod. Phys.*, vol. 74, pp. 145–195, 1 Mar. 2002. DOI: 10.1103/RevModPhys.74.145.
- [2] V. Scarani, H. Bechmann-Pasquinucci, N. J. Cerf, M. Dusek, N. Lutkenhaus, and M. Peev, "The security of practical quantum key distribution", *Rev. Mod. Phys.*, vol. 81, pp. 1301–1350, 3 Sep. 2009. DOI: 10.1103/RevModPhys.81.1301.
- [3] L. K. Grover, "Quantum mechanics helps in searching for a needle in a haystack", *Physical review letters*, vol. 79, no. 2, p. 325, 1997.
- [4] P. W. Shor, "Polynomial-time algorithms for prime factorization and discrete logarithms on a quantum computer", *SIAM review*, vol. 41, no. 2, pp. 303–332, 1999.
- [5] P. Townsend, "Simultaneous quantum cryptographic key distribution and conventional data transmission over installed fibre using wavelength-division multiplexing", *Electronics Letters*, vol. 33, pp. 188–190(2), 3 Jan. 1997.
- [6] L.-J. Wang, K.-H. Zou, W. Sun, *et al.*, "Long-distance copropagation of quantum key distribution and terabit classical optical data channels", *Phys. Rev. A*, vol. 95, p. 012301, 1 Jan. 2017. DOI: 10.1103/PhysRevA.95.012301.
- [7] Y. Mao, B.-X. Wang, C. Zhao, *et al.*, "Integrating quantum key distribution with classical communications in backbone fiber network", *Opt. Express*, vol. 26, no. 5, pp. 6010–6020, Mar. 2018. DOI: 10.1364/OE.26.006010.
- [8] J.-Q. Geng, G.-J. Fan-Yuan, S. Wang, *et al.*, "Coexistence of quantum key distribution and optical transport network based on standard single-mode fiber at high launch power", *Opt. Lett.*, vol. 46, no. 11, pp. 2573–2576, Jun. 2021. DOI: 10.1364/OL.426175.
- [9] J.-Q. Geng, G.-J. Fan-Yuan, S. Wang, *et al.*, "Quantum key distribution integrating with ultra-high-power classical optical communications based on ultra-low-loss fiber", *Opt. Lett.*, vol. 46, no. 24, pp. 6099–6102, Dec. 2021. DOI: 10.1364/OL.446939.
- [10] P. Gagnon, F. Mondain, E. Pincemin, *et al.*, "Co-propagation of 6 tb/s (60\*100gb/s) dwdm & qkd channels with 17 dbm aggregated wdm power over 50 km standard single mode fiber", *Conference on Optical Fiber Communications (OFC)*, no. Tu3H.2, 2023.
- [11] B. Qi, W. Zhu, L. Qian, and H.-K. Lo, "Feasibility of quantum key distribution through a dense wavelength division multiplexing network", *New Journal of Physics*, vol. 12, no. 10, p. 103042, Oct. 2010. DOI: 10.1088/1367-2630/12/10/103042.
- [12] N. A. Peters, P. Toliver, T. E. Chapuran, *et al.*, "Dense wavelength multiplexing of 1550 nm qkd with strong classical channels in reconfigurable networking environments", *New Journal of Physics*, vol. 11, no. 4, p. 045012, Apr. 2009. DOI: 10.1088/1367-2630/11/4/045012.
- [13] T.-Y. Chen, J. Wang, H. Liang, *et al.*, "Metropolitan all-pass and inter-city quantum communication network", *Opt. Express*, vol. 18, no. 26, pp. 27217–27225, Dec. 2010. DOI: 10.1364/OE.18.027217.
- [14] L.-J. Wang, L.-K. Chen, L. Ju, *et al.*, "Experimental multiplexing of quantum key distribution with classical optical communication", *Applied Physics Letters*, vol. 106, no. 8, p. 081108, 2015. DOI: 10.1063/1.4913483.
- [15] P. Eraerds, N. Walenta, M. Legre, N. Gisin, and H. Zbinden, "Quantum key distribution and 1 gbps data encryption over a single fibre", *New Journal of Physics*, vol. 12, no. 6, p. 063027, Jun. 2010. DOI: 10.1088/1367-2630/12/6/063027.
- [16] K. A. Patel, J. F. Dynes, I. Choi, *et al.*, "Coexistence of high-bit-rate quantum key distribution and data on optical fiber", *Phys. Rev. X*, vol. 2, p. 041010, 4 Nov. 2012. DOI: 10.1103/PhysRevX.2.041010.
- [17] K. A. Patel, J. F. Dynes, M. Lucamarini, *et al.*, "Quantum key distribution for 10 gb/s dense wavelength division multiplexing networks", *Applied Physics Letters*, vol. 104, no. 5, p. 051123, 2014. DOI: 10.1063/1.4864398.
- [18] I. Choi, Y. R. Zhou, J. F. Dynes, *et al.*, "Field trial of a quantum secured 10 gb/s dwdm transmission system over a single installed fiber", *Opt. Express*, vol. 22, no. 19, pp. 23121–23128, Sep. 2014. DOI: 10.1364/OE.22.023121.
- [19] J. F. Dynes, W. W. Tam, A. Plews, *et al.*, "Ultra-high bandwidth quantum secured data transmission", *Nature Scientific reports*, vol. 6, no. 1, p. 35149, 2016. DOI: 10.1038/srep35149.
- [20] I. Lucio-Martinez, P. Chan, X. Mo, S. Hosier, and W. Tittel, "Proof-of-concept of real-world quantum key distribution with quantum frames", *New Journal of Physics*, vol. 11, no. 9, p. 095001, Sep. 2009. DOI: 10.1088/1367-2630/11/9/095001.
- [21] Z. Tang, Z. Liao, F. Xu, B. Qi, L. Qian, and H.-K. Lo, "Experimental demonstration of polarization encoding measurement-device-independent quantum key distribution", *Phys. Rev. Lett.*, vol. 112, p. 190503, 19 May 2014. DOI: 10.1103/PhysRevLett.112.190503.
- [22] E. Moschandreou, B. J. Rollick, B. Qi, and G. Siopsis, "Experimental decoy-state bennett-brassard 1984 quantum key distribution through a turbulent channel", *Phys. Rev. A*, vol. 103, p. 032614, 3 Mar. 2021. DOI: 10.1103/PhysRevA.103.032614.
- [23] X. Ma, B. Qi, Y. Zhao, and H.-K. Lo, "Practical decoy state for quantum key distribution", *Phys. Rev. A*, vol. 72, p. 012326, 1 Jul. 2005. DOI: 10.1103/PhysRevA.72.012326.